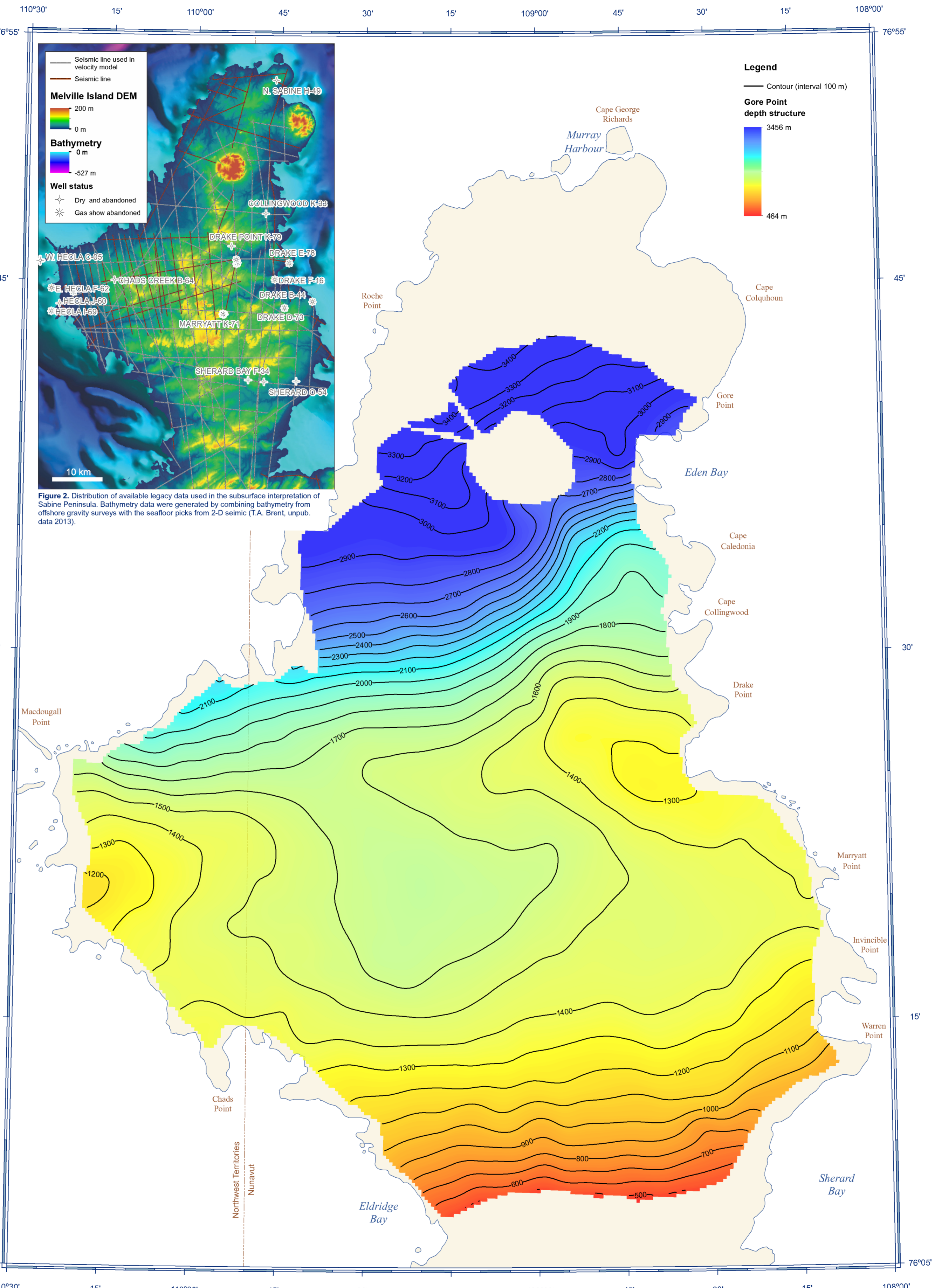


**Legend**  
 Contour (interval 50 m)  
**Gore Point time structure**  
 2281 ms  
 170 ms

Figure 1. Generalized surface geology map of Sabine Peninsula (after Harrison, 1994) displaying sedimentary stratigraphic divisions.



**Legend**  
 Contour (interval 100 m)  
**Gore Point depth structure**  
 3456 m  
 464 m

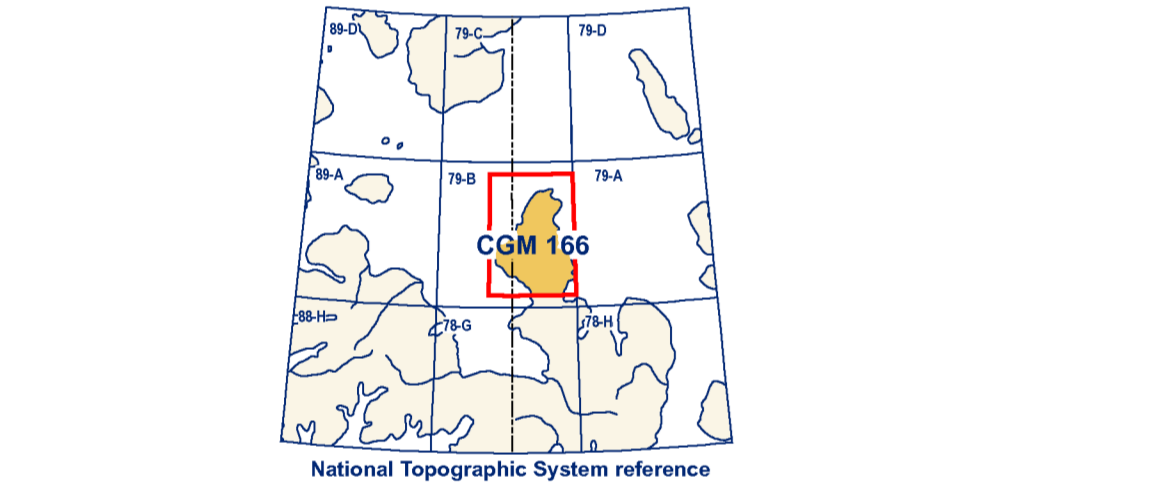
Figure 2. Distribution of available legacy data used in the subsurface interpretation of Sabine Peninsula. Bathymetry data were generated by combining bathymetry from offshore gravity surveys with the seafloor picks from 2-D seismic (A. Brent, unpub. data 2013).

**Abstract**  
 Sabine Peninsula of Melville Island was the subject of an oil and gas exploration boom from 1981 to 1985, during which time seismic-reflection data were collected and wells were drilled. As a result, the two largest conventional natural gas fields in Canada were discovered.

**Résumé**  
 La péninsule de Sabine de l'île de Melville a connu un boom d'exploration gazière et pétrolière entre 1981-1985 pendant lequel des données de sismique-réflexion furent acquises et des puits forés. Il en résulta la découverte des deux plus grands champs de gaz naturel conventionnels du Canada.

Seismic-reflection methods use sound waves to image the internal structure of the Earth. Waves are emitted at the surface before being reflected back to the surface by geological interfaces and recorded. Modern analysis methods were used to re-investigate existing seismic data. In doing so, eight seismic unit boundaries identified on seismic profiles in two-way time were correlated to the regional geological framework and gridded to provide subsurface maps. Each map approximates the structures preserved at that particular time or depth allowing the enhancement of the geological knowledge of Sabine Peninsula and better delineation of elements of the petroleum systems therein.

Les méthodes de sismique-réflexion utilisent des ondes sonores pour imaginer la structure interne de la Terre. Les ondes sont émises en surface avant d'être réfléchies de nouveau vers la surface par des interfaces géologiques et enregistrées. Des méthodes d'analyse modernes furent utilisées pour ré-investiger des données sismiques existantes. Ainsi, huit limites d'unités sismiques identifiées sur les profils sismiques en temps de parcours aller-retour furent corrélées au cadre géologique régional et maillées afin de produire des cartes de la sous-surface. Chaque carte est une approximation des structures préservées à un certain temps ou une certaine profondeur nous permettant d'améliorer la connaissance géologique de la péninsule de Sabine et de mieux délimiter les éléments des systèmes pétroliers s'y trouvant.



Catalogue No. M163-1196-2013E-PDF  
 ISBN 978-1-105-2924-8  
 doi:10.4095/29300

Natural Resources Canada / Ressources naturelles du Canada

**CANADIAN GEOSCIENCE MAP 166**  
**TIME- AND DEPTH-STRUCTURE MAP**  
**GORE POINT MEMBER**  
**ROCHE POINT FORMATION**

Sabine Peninsula, Melville Island  
 Nunavut-Northwest Territories  
 1:200 000



ess.nrcan.gc.ca

**Authors:** M.J. Duchesne, V.I. Brake, K. Dewing, M. Claprood, E. Gloaguen, and T.A. Brent  
**Geomatics by:** V.I. Brake, Geological Survey of Canada and G. Huot-Vézina, Institut national de la recherche scientifique  
**Cartography by:** R. Boivin  
**Scientific editing by:** E. Inglis  
**Initiative of the Geological Survey of Canada, conducted under the auspices of the Western Arctic Islands' project as part of Natural Resources Canada's Geo-mapping for Energy and Minerals (GEM) program.**

Map projection: Universal Transverse Mercator, zone 12  
 Base map at the scale of 1:280 000 from Natural Resource Canada, with modifications.  
 Proximity to the North Magnetic Pole causes the magnetic compass to be useless in this area.

The Geological Survey of Canada welcomes corrections or additional information from users.  
 The data may include additional observations not portrayed on this map. See documentation accompanying the data.  
 This publication is available for free downloading through GEOCAN (http://geocan.ess.nrcan.gc.ca/).  
 This map is not to be used for navigational purposes.

**TIME- AND DEPTH-STRUCTURE MAP**  
**GORE POINT MEMBER**  
**ROCHE POINT FORMATION**

Sabine Peninsula, Melville Island  
 Nunavut-Northwest Territories  
 1:200 000

**DESCRIPTIVE NOTES**

**INTRODUCTION**  
 The time- and depth-structure maps presented herein are part of an eight-map series of the subsurface of Sabine Peninsula spanning the Early Permian through Early Cretaceous interval. These maps are the product of the application of modern geoscientific methods of processing and interpretation to a suite of legacy seismic-reflection data from onshore Sabine Peninsula (Melville Island, Western Arctic Islands). The resultant processed seismic lines were interpreted using the existing regional geological framework (see Harrison, 1995) by integrating existing regional well data, geological logs, age control, and lithological information through synthetic seismograms.

**REGIONAL SETTING**  
 The Sabine Peninsula of Melville Island is located within the Sverdrup Basin in the Queen Elizabeth Islands of the western Arctic. The Sverdrup Basin extends for about 1300 km in a north-south-southwest direction and is up to 250 km wide. The basin contains up to 13 km of sedimentary strata (Embry and Beauchamp, 2008). The Sverdrup Basin is separated from the underlying Franklinian Basin by an unconformity at the base of the Carboniferous strata. The Franklinian Basin was extensively redeformed during the Late Devonian-earliest Carboniferous Eiseismitic Orogeny. The resulting rift-related structural depression acted as a major depositor for the Carboniferous through the Paleogene (Embry and Beauchamp, 2008). The Sverdrup Basin succession was uplifted and deformed during the early Cenozoic Eurasian Orogeny.

The surface geology of Melville Island is dominated by Lower Paleozoic strata of the Franklinian Basin. The Sabine Peninsula is an exception to this, as surface strata are part of the Sverdrup Basin. The geology of the Sabine Peninsula consists of deformed Late Carboniferous to Paleocene sandstone, siltstone, shale, and minor amounts of carbonate. Additionally, evaporite, rocks are exposed in two diapirs on northern Sabine Peninsula—the Barrow and Colquhoun domes, which consist of deformed anhydrite and gypsum. The strata of the Sverdrup Basin succession on Melville Island were deformed into a series of folds, including the Murray Point syncline in the northern part of the peninsula and the Drake Point anticline and the Maryatt Point syncline to the south (Harrison, 1994) (Fig. 1).

**SEISMIC DATA SET AND PROCESSING**  
 Data access was obtained through a Memorandum of Understanding signed in 1997 by the Geological Survey of Canada (GSC), Panarctic Oils, the Arctic Islands Exploration Group, and the Western Arctic Exploration Group venture parties. The data sets consist of original land seismic-reflection field tapes transferred from 21-, 7-, and 9-track media. Data were collected using a dynamic charge of 25–30 kg per shot at about 20 m below the surface, shotpoint spacing ranged from 67 m to 300 m, the shorter spacing being used for most surveys. The primary seismic-reflection data were recorded using 48- or 96-channel systems. Channel stations were generally deployed using nine receivers spaced at about 8 m and station intervals varying from 50 m to 70 m. The common-midpoint multiplicity of the data sets range from single to 12-fold coverage. The most common recording length was 6 s.

The processing consisted of three main steps: (1) principal component decomposition was used to remove both coherent and random noise; (2) data were migrated utilizing poststack Kirchhoff migration; and (3) seismic bandpasses were extended to increase vertical resolution (Claprood et al., 2011; Duchesne et al., 2012).

**Velocity model**  
 A 3-D velocity model was built using about 1300 km of linear seismic data (78 lines) and 13 wells spread over an area of about 2800 km<sup>2</sup> (Fig. 2). The velocity model was then used for poststack migration processing and to convert seismic horizon surfaces from time to depth. The primary assumption behind the velocity model is that the coherent high-amplitude reflections that were picked to build the model correspond to important acoustic impedance contrasts caused by significant and abrupt velocity changes. This assumption was confirmed by tying seismic picks to well sonic logs (Duchesne et al., 2012). The geostatistical approach of kriging with an external drift (KED) was applied to both the reflection time of the picked seismic horizons and time-depth pairs derived from check shot data to compute the 3-D velocity field. Kriging interpolates values between the known positions based on weighted spatial correlations. The KED technique was specifically developed for the integration of seismic data into the kriging process where the number of wells is insufficient for the computation of adequate depth statistics (Haas and Dubrule, 1994). Hence, it uses the information provided by the time horizon picks to improve estimates where depth control is sparse. For seismic migration, root-mean squared (RMS) velocity values are first estimated by KED from time-to-depth conversion of seismic horizon surfaces mapped as important velocity boundaries (Duchesne et al., 2012). Then, once the approximate depths of the surfaces are known, the interval velocities ( $V_{int}$ ) for all time intervals delimited by two consecutive horizons is computed from:

$$V_{int} = \frac{\Delta z_i}{\Delta t_i}$$

where  $\Delta z_i$  and  $\Delta t_i$  are the depth and time intervals between two successive horizons  $i$ . Once  $V_{int}$  is obtained the RMS velocity ( $V_{rms}$ ) is calculated using:

$$V_{rms} = \sqrt{\frac{1}{t_0} \sum_{i=1}^N V_{int}^2 \Delta t_i}$$

in which  $N$  is the total number of horizons and  $t_0$  is the sum of all time intervals.

**SEISMIC INTERPRETATION AND VISUALIZATION METHODS**  
 Processed seismic lines were loaded into IHS-Kingdom<sup>®</sup> seismic and geological interpretation software. Prominent seismic-reflection horizons, tied to well formation-top information, were manually correlated. Seed points were generated at seismic line intersections, thereby permitting the interpretation of acorlines.

The map would benefit from a detailed structural interpretation; however, confidence of this interpretation is minimized due to minor vertical offsets (about 0.1 s) attributed to heaving and the large line spacing. Thus reflections are readily identified across faults despite offset.

Time-structure maps of the key seismic horizons were computed using universal kriging. Universal kriging permits the interpolation of a nonstationary random field by adding a term in the kriging equation that accommodates any linear trends present in a scattered point set (Chilès and Dubrule, 1999). Given that all picked horizons showed a strong linear trend for time versus depth over distance, universal kriging provided the best fit to the picked horizons.

**TIME TO DEPTH CONVERSION**  
 All time surfaces were converted to depth using the following procedure. First  $V_{int}$  of the 3-D velocity model are calculated using Dix equation:

$$V_{int} = \left[ \frac{V_{rms}^2(t_n) - V_{rms}^2(t_{n-1})}{t_n - t_{n-1}} \right]^{1/2}$$

where  $t$  is the zero-offset arrival time of the  $n$ th reflection. Interval limits corresponded to seismic horizons that are picked and tied to geological interfaces. Then  $V_{int}$  are extracted from the velocity model along picked horizons. Velocity maps are then computed using Universal kriging at a cell size of 250 m. Finally, the time-structure surfaces of the various seismic horizons are converted to depth ( $Z$ ) using:

$$Z = \frac{t_n - t_0}{2}$$

Because the depth-conversion process is a function of the velocity model, the lateral extent of depth maps is confined to the lateral extent of the model. The final depth-structure maps were imported into ArcGIS for visualization using the Arc extension Team-GIS Bridge.

**Recommended citation**  
 Duchesne, M.J., Brake, V.I., Dewing, K., Claprood, M., Gloaguen, E. and Brent, T.A., 2013. Time- and depth-structure maps of the Gore Point Member, Roche Point Formation, Sabine Peninsula, Melville Island, Nunavut-Northwest Territories. Geological Survey of Canada, Canadian Geoscience Map 166, scale 1:200 000. doi:10.4095/29300

**UNCERTAINTY**

Quantifying the uncertainty of seismic subsurface maps is difficult since several sources of data, each with their unique level of uncertainty, are used in the map generation. Sources of error may arise from limitations in acquisition, processing, and interpretation. Moreover, seismic data are collected remotely and the images they provide are derived from generalized mathematical and physical concepts. Common sources of error in acquisition that increase the uncertainty include gaps in coverage because of obstacles to source and receiver deployment, and effect of direction of shooting on data quality (Sheriff and Geldart, 1995). Processing errors may result from inadequate static corrections, inaccurate velocity analysis, and inappropriate parameter determination.

More recently to this data set, errors may have also been introduced by the velocity model and the ability to tie formation tops to seismic horizons. The velocity model represents an estimation of the velocity fluctuations for which the accuracy depends on the number of wells and the good fit between time picks and corresponding depths at the well locations. A regression analysis shows that time picks and their corresponding depths at the wells have a strong linear fit ( $r^2 = 0.98$ ), meaning that the use of time picks as the external drift in the kriging strategy is justified and satisfactory. Nevertheless, the uncertainty of the velocity model increases when the distance between the well and any points where velocity is predicted exceed the range of the varying geospatial dependence between depth and time in the present case, the range of the different horizons is between 9.5 km and 34 km.

The ability to tie formation tops to seismic horizons relies on the successful use of well sonic and density logs, since it is the contrast between the product of these properties for two successive geological layers that generates reflections recorded in seismic exploration. Formation tops used in this study are from Dewing and Embry (2007), for which they mainly utilized gamma-ray logs to position the upper limit of the formations in depth. Thus errors may have been introduced by projecting the formation tops on seismic sections recorded in time.

**TIME- AND DEPTH-STRUCTURE DATA DISPLAY**

The time- and depth-structure data shown on this map were gridded at a cell size of 250 m using Universal kriging. Each map presents a grid with a stretched colour ramp at 20% transparency. Time contours generated from the time-structure grids are shown in black at a 50 ms interval, whereas depth contours derived from the depth-structure grid are presented at 100 m intervals.

**GORE POINT MEMBER DESCRIPTIONS**

The Late Triassic Gore Point Member of the Roche Formation, Schei Point Group consists of carbonates, with local gypsum and mudrock (Dewing and Embry, 2007; see also Fig. 3). The Schei Point Group is divided into five formations: Murray Harbour, Roche Point, Hoyle Bay, Pat Bay, and Barrow (Embry, 1984a). Further to this division, the Roche Point Formation is separated into four members: Eldridge Bay, Cape Caladonia, Chads Point, and Gore Point (Embry, 1984a). The Gore Point Member is commonly referred to as the Gore Point limestone. According to formation-top information from the Sabine Peninsula, the Gore Point Member overlies the Chads Point Member of the same formation and is overlain by the Eden Bay Member of the Hoyle Bay Formation, Schei Point Group (Dewing and Embry, 2007).

The mapped Gore Point Formation reflection extends from the Eldridge-Sherard Bay area to the northern part of the peninsula. The dip gap west of Eden Bay marks the location of Barrow Dome. Two-way traveltimes of the Gore Point Formation reflection increase northward from 170 ms to 2281 ms or from 464 m to 3456 m. The slope of the Gore Point Member-Roche Point horizon averages 2°. The observed slopes are observed north of the Drake Point anticline and in the southern part of Sabine Peninsula where they approach 8°. The primary slope azimuth of this horizon is north. A notable depression lies at the centre of Sabine Peninsula delimited by the Drake Point anticline to the north and the Maryatt Point syncline to the south (Harrison, 1994).

Wiggle plot (ms)	Synthetic Rock	Age	Formation
67	tr	Triassic	Invincible Mt. Member, Christopher Fm.
14	tr	Triassic	Christopher section, Christopher Fm.
21	tr	Triassic	Haadsen Fm.
28	tr	Triassic	Ailingak Fm.
14	tr	Triassic	Prominent reflection Ailingak Fm.
14	tr	Triassic	Sandy Point Fm.
21	tr	Triassic	Grossverand Island Fm.
21	tr	Triassic	Gore Point Mb., Roche Point Fm.
21	tr	Triassic	Degehorls Fm.
21	tr	Triassic	Great Bear Cape Fm.

Figure 3. Comparison of the wiggle plot, synthetic trace, stratigraphy, age, and formation-top data for the Chads Creek B-64 well.

**ACKNOWLEDGMENTS**

The authors would like to thank J. Dietrich and B. MacLean (GSC Calgary) for their technical reviews that improved the overall quality of the maps. IHS is acknowledged for providing Kingdom 8.8 seismic interpretation software.

**REFERENCES**

Chilès, J.-P. and Delfiner, P., 1999. Geostatistics: Modeling Spatial Uncertainty. Wiley Series in Probability and Statistics. Wiley, New York, 734 p.

Claprood, M., Duchesne, M.J., and Gloaguen, E., 2011. A geostatistical approach for 2-D seismic velocity modelling. Geological Survey of Canada, OpenFile 7045, 21 p. doi:10.4095/289951

Dewing, K. and Embry, A.F., 2007. Geological and geochemical data from the Canadian Arctic Islands. Part I: Stratigraphic logs from Arctic Islands of all gas exploration basins. Geological Survey of Canada, Open File 5442, 142-PCM. doi:10.4095/22386

Duchesne, M.J., Claprood, M., and Gloaguen, E., 2012. Improving seismic velocity estimation for 2D poststack time migration of regional seismic data using kriging with an external drift. The Leading Edge, v. 31, p. 1158–1166.

Embry, A.F., 1984a. The Schei Point and Baa Mourain Groups (Middle-Upper Triassic), Sverdrup Basin, Canadian Arctic Archipelago. In: Current Research, Part B. Geological Survey of Canada, Paper 84-16, p. 327–338. doi:10.4095/119589

Embry, A.F., 1984b. Stratigraphic subdivision of the Roche Point, Hoyle Bay and Barrow Formations (Schei Point Group), western Sverdrup Basin, Arctic Islands. In: Current Research, Part B. Geological Survey of Canada, Paper 84-16, p. 275–283. doi:10.4095/119583

Embry, A. and Beauchamp, E., 2008. Sverdrup Basin: In Sedimentary Basins of the World, (ed. K.J. Halv), Volume 5: The Sedimentary Basins of the United States and Canada. Elsevier, Amsterdam, The Netherlands, p. 451–471.

Harrison, J.C., 1994. Melville Island and adjacent smaller islands, Canadian Arctic Archipelago, District of Franklin, Northwest Territories. Geological Survey of Canada, Map 1944A, scale 1:250 000. doi:10.4095/20377

Harrison, J.C., 1995. Melville Island's salt-based fold belt, Arctic Canada. Geological Survey of Canada, Bulletin 472, 34 p. doi:10.4095/29376

Haas, A. and Dubrule, O., 1994. Geostatistical inversion – a sequential method of stochastic reservoir modelling constrained by seismic data. First Break, v. 12, p. 961–969.

Sheriff, R.E. and Geldart, L.P., 1995. Exploration Seismology. Cambridge University Press, New York, New York, 629 p.